ACS OMEGA

http://pubs.acs.org/journal/acsodf

Article

Ethanedihydrazide as a Corrosion Inhibitor for Iron in 3.5% NaCl Solutions

Ayman H. Ahmed,* El-Sayed M. Sherif, Hany S. Abdo, and Ehab Said Gad

Cite This: *ACS Omega* 2021, 6, 14525−14532

Read Online

ACCESS | Metrics & More | Article Recommendations

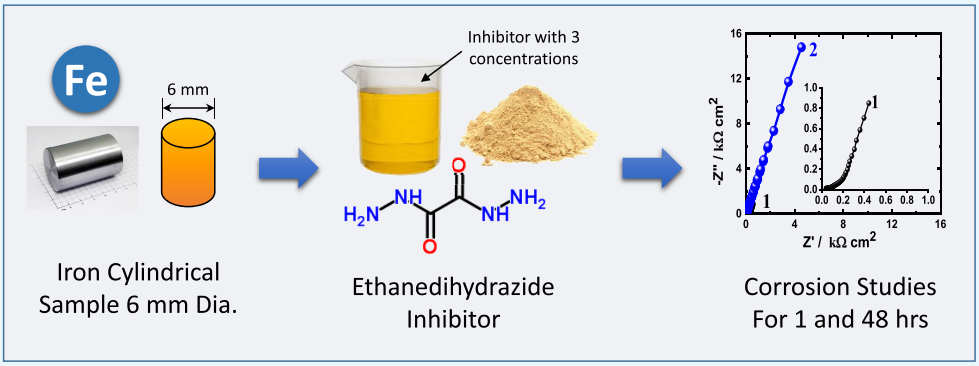

ABSTRACT: Corrosion of iron in sodium chloride (3.5% wt) solutions and its inhibition by ethanedihydrazide (EH) have been reported. Electrochemical impedance spectroscopy (EIS), cyclic potentiodynamic polarization (CPP), and change of current with time at −475 mV (Ag/AgCl) measurements were employed in this study. Scanning electron microscopy (SEM) and energy-dispersive X-ray (EDX) techniques were utilized to report surface morphology and elemental analysis, respectively. The presence of 5×10^{-5} M EH was found to inhibit the corrosion of iron, and the effect of inhibition profoundly increased with an increase in EH concentration up to 1×10^{-4} M and further to 5×10^{-4} M. The low values of corrosion current and high corrosion resistance, which were obtained from the EIS, CPP, and change of current with time experiments, affirmed the adequacy of EH as a corrosion inhibitor for iron. Surface investigations demonstrated that the chloride solution without EH molecules causes severe corrosion, while the coexistence of EH within the chloride solution greatly minimizes the acuteness of chloride, particularly pitting corrosion.

1. INTRODUCTION

Corrosion of metals is a major problem since it costs many billion dollars annually. The physiochemical interaction between a metal and its environment leads to variations in the properties of the metal, which may affect the function of the metal. Therefore, inhibition of metal corrosion is of paramount importance owing to the utilization of metals in various fields of innovation. Although metals are not completely safe from corrosion, we can prevent corrosion to some extent in metals. For this reason, corrosion inhibitors are used to interact with a metal surface and hence prevent metal corrosion. Iron metal and its numerous alloys are considered the most important materials as they have numerous practical applications. Iron is used to make alloys in addition to the manufacture of ships, rails, bridges, pipes, boilers, reinforcement steel, etc. Interestingly, iron corrosion causes a loss of one-fourth of world's production in a year and this is an economic catastrophe.

According to the literature, many organic and inorganic compounds are utilized as inhibitors in controlling the corrosion of metals in 3.5% NaCl. Among these inorganic inhibitors, sodium molybdate, cerium nitrate, and Ce(III, IV) ammonium nitrate have been employed as corrosion inhibitors for steel pipelines,[1] mild steel (MS),[2] and AA2024 aluminum alloy,[3] respectively. In the context of preservation of different metals in 3.5% NaCl brine solution using organic inhibitors, many substances have been evaluated. Macedo et al. studied the inhibition mechanism of imidazole and some of its derivatives onto an iron surface in 3.5% NaCl medium.[4] The outcomes showed that the considered compounds act as anodic corrosion inhibitors for iron in saline medium. Aslam et al. investigated the inhibitory behavior of *N*,*N*′-didodecyl-*N*,*N*′-digluconamideethylenediamine gemini surfactant on mild steel (MS) corrosion in 3.5% NaCl at 30−60 °C.[5] The compound mitigated corrosion, and the degree of inhibition was dependent on

Received: March 22, 2021
Accepted: May 13, 2021
Published: May 27, 2021

concentration and temperature. Moreover, 3-amino-5-mercapto-1,2,4-triazole,[6] 5-(3-aminophenyl)-tetrazole,[7] 1,1′-thiocarbonyldiimidazole,[8] sodium 2-(4-(benzo[*d*]thiazol-2-ylthio)-6-(hexylamino)-1,3,5-triazin-2-ylamino) ethanesulfonate,[9] hexamine,[10] (3-amino-1,2,4-triazole-5-thiol and 1,1′-thiocarbonyldiimidazole),[11] (2-sulfhydryl)-(5-phenmethyl)-(1-(4-phenol)-methanimine)-triazole,[12] poly(ethyleneimine),[13] 1-butyl-3-methylimidazolium chloride,[14] and cetylpyridinium chloride[15] have been examined as corrosion inhibitors for different metals, especially iron species, in the same medium.

Although the previously mentioned inhibitors have an excellent corrosion inhibition efficiency, their high cost encourages researchers to look for alternative sources. For this reason, plant extracts/natural materials are chosen to restrain corrosion of metals because of their low cost, safety, and easy accessibility; moreover, they are environmentally friendly and biodegradable. Othman et al. examined the inhibition efficiency of rice straw extract for steel in 3.5% NaCl.[16] Suarez et al. investigated the inhibition effect of mango extract as a corrosion inhibitor on carbon steel by varying the pH of the electrolytic medium.[17] Furthermore, the corrosion inhibition performance of apple pomace,[18] *Elettaria cardamomum*,[19] and *Myrmecodia pendans*[20] for C1010 steel, mild steel, and carbon steel, respectively, was evaluated in 3.5% NaCl medium and the accomplishments proved the effectiveness of these materials.

It is reported that efficient inhibitors are those compounds that contain heteroatoms like O, N, S, and P, which cause physical/chemical adsorption on metal surfaces.[21,22] The inhibition performance of these compounds is enhanced in the order O < N < S < P.[23−25] In continuation of previous work on examining some N- and O-containing organic inhibitors,[26−29] the authors have considered the corrosion inhibiting behavior of a hydrazide, namely, ethanedihydrazide (EH) (Figure 1), on iron corrosion in an NaCl solution. Although

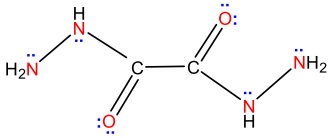

Figure 1. Structure of ethanedihydrazide (EH).

some reports have documented the use of hydrazides as corrosion impeding agents for some iron species such as *N*′[(1E)-(4-hydroxyphenyl)methylene]isonicotinohydrazide and *N*′-[(1E)-(4-hydroxy-3-methoxyphenyl)methylene]-isonicotinohydrazide,[30] hydroxyphenylhydrazide,[31] sulfonohydrazide derivatives,[32] and pyrazine carbohydrazide,[33] the corrosion inhibition ability of ethanedihydrazide for iron in neutral chloride medium (3.5% NaCl) has not been achieved up to now. It is noteworthy that the molecular structures of many reported inhibitors that slow down the corrosion rate of metals in a 3.5% NaCl environment often contain N and/or O heteroatoms and π-bonds (particularly as NH, C═O, and NH_2 functional groups) analogous to the molecular structure of the studied inhibitor. Surely, the inhibition property of EH is attributed to its adequate chemical structure. The lone pairs of electrons on the heteroatoms (N, O) and the existence of π bonds in the entire structure, besides its ability to chelate with metals,[34] are assumed to be significant factors that induce the adsorption of this molecule on an iron surface.

In view of the inhibitive impact of organic compounds containing N and O heteroatoms, we examined the effect of ethanedihydrazide (EH) on iron corrosion in aerated 3.5% NaCl solutions employing various electrochemical strategies. The cathodic, anodic, and corrosion currents, corrosion potential, corrosion rate, and corrosion resistance of iron were assessed from the polarization data. Electrochemical impedance spectroscopy (EIS) experiments were performed to report Nyquist plots as well as the values of polarization resistances. The absolute flow currents and the influence of tested samples on corrosion inhibition were determined from the chronoamperometric current versus time runs. Scanning electron microscopy (SEM) analysis was performed to portray the surface morphology of iron metal after corrosion process. Energy-dispersive X-ray (EDX) techniques were used to detect the composition of the adsorbed layer on the iron surface in the absence and presence of the EH inhibitor.

2. EXPERIMENTAL SECTION

2.1. Chemicals and the Electrochemical Cell. Ethanedihydrazide (EH) was supplied by Sigma-Aldrich. NaCl salt (99% purity) was delivered by Merck. A high-purity iron rod (99.99%) with an area of 0.25 cm^2 was purchased from Goodfellow (Ermine Business Park, Huntingdon, England) and was used as the working electrode in this work. Electrochemical measurements were performed in a traditional three-electrode electrochemical cell that can accommodate 0.250 L of solution. A Pt sheet and a silver−silver chloride (Ag/AgCl) electrode were employed as the counter and reference electrodes, respectively. The iron working electrode was prepared and employed to obtain corrosion results as reported in previous studies.[35,36] EH powder was dissolved in dimethylformamide (DMF) to prepare a stock solution of 0.01 M EH. A stock solution of 7% NaCl was prepared by dissolving 70 g of powdered sodium chloride (NaCl) in 1000 mL of bidistilled water. The desired chloride solutions without and with EH molecules were synthesized from the stock solutions by dilution.

2.2. Surface Electrochemical Strategies and Characterization. The electrochemical experiments were measured using a PGSTAT302N Autolab that was delivered by Metrohm. The EIS data were obtained at the open-circuit potential value with frequency ranging from 100 MHz to 100 mHz. The impedance measurements were obtained via applying a ±5 mV amplitude sinusoidal wave perturbation. The polarization investigations (cyclic potentiodynamic polarization (CPP)) were carried out by scanning the potential from −1200 to +100 mV (Ag/AgCl) with a scanning rate of 1.66 mV/s. The current−time experiments were performed for the iron rod by stepping the potential to −475 mV for 1 h. The SEM micrographs and EDX investigations were collected using a JEOL microscope with an EDX unit attached; the machine operated at 15 kV. All experiments were performed in triplicate on a newly polished surface of iron with a fresh test solution at a temperature of 25 ± 3 °C.

3. RESULTS AND DISCUSSION

3.1. Electrochemical Impedance Spectroscopy. The EIS technique was employed to report corrosion and corrosion inhibition processes.[37,38] Nyquist plots for the iron rod after (1) 1 and (2) 48 h immersion in (a) 3.5% blank NaCl solution and 3.5% NaCl solutions with (b) 5×10^{-5}, (c) 1×10^{-4}, and (d) 5×10^{-4} M EH are shown in Figure 2. It was observed that the

https://doi.org/10.1021/acsomega.1c01422
ACS Omega 2021, 6, 14525−14532

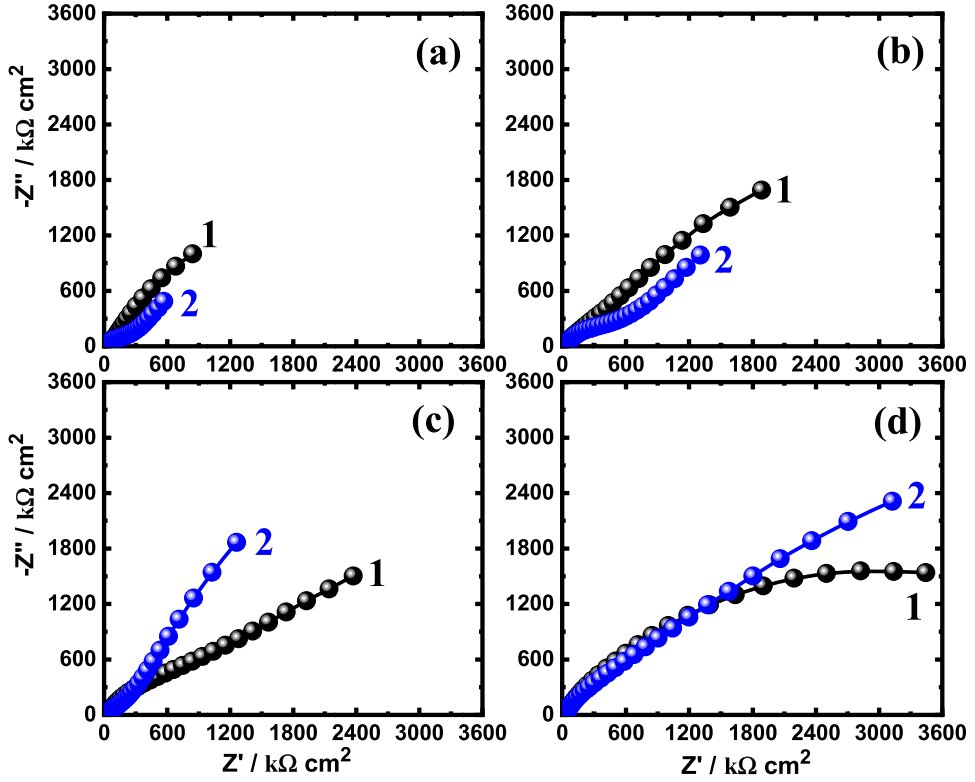

Figure 2. Nyquist plots for the iron rod after (1) 1 h and (2) 48 h immersion in (a) 3.5% blank NaCl solution and 3.5% NaCl solutions with (b) 5×10^{-5} M EH, (c) 1×10^{-4} M EH, and (d) 5×10^{-4} M EH.

spectrum obtained for iron in the blank chloride solution (Figure 2a) had the lowest diameter for the obtained semicircle. Mixing 5×10^{-5} M EH with chloride solutions (Figure 2b) resulted in a wider diameter of the plotted semicircle; this effect was enhanced on adding higher concentrations of EH, 1×10^{-4} M and further 5×10^{-4} M.

The experimental data were fitted to an equivalent circuit that is exhibited in Figure 3. The symbols of the circuit can be defined as follows: a solution resistance (R_S), constant phase elements (CPEs, Q), and a polarization resistance (R_P). The values of these parameters were determined for the iron rod in all tested solutions, in addition to the inhibition efficiency percentage (IE/%) for the EH compound (shown in Table 1). The IE% values were obtained as follows[39−44]

$$\mathrm{IE\%} = \frac{R_P^{in} - R_P^{o}}{R_P^{o}} \times 100 \quad (1)$$

Here, R_P^{o} and R_P^{in} are the polarization resistances for the iron rod in chloride solutions without and with EH inhibitor molecules present, respectively.

The Nyquist plots in Figure 2 reveal that the addition and increment of EH concentration minimize the corrosion impact of NaCl solution via inhibiting the deterioration of the iron rod. This can be deduced from the breadths of the semicircle in the Nyquist plots for 3.5% NaCl solution with EH. The values recorded in Table 1 also ascertain that the presence of EH

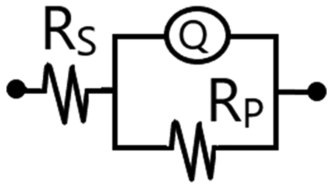

Figure 3. Circuit model that fits the impedance data.

Table 1. Values of EIS Parameters and IE% for Iron in 3.5% NaCl without and with EH

		Q (CPEs)			
parameter (solution)	R_s (Ω cm^2)	Y_Q (F/cm^2)	n	R_P (Ω cm^2)	IE (%)
3.5% NaCl + 0.0 M EH (1 h)	9.65	7.45×10^{-6}	0.86	655	
3.5% NaCl + 5×10^{-5} M EH (1 h)	10.23	6.55×10^{-6}	0.89	1231	46.82
3.5% NaCl + 1×10^{-4} M EH (1 h)	10.91	6.02×10^{-6}	0.91	1974	66.84
3.5% NaCl + 5×10^{-4} M EH (1 h)	11.54	5.72×10^{-6}	0.93	3259	79.91
3.5% NaCl + 0.0 M EH (48 h)	10.13	7.23×10^{-6}	0.82	691	
3.5% NaCl + 5×10^{-5} M EH (48 h)	10.86	6.77×10^{-6}	0.86	1484	53.43
3.5% NaCl + 1×10^{-4} M EH (48 h)	11.44	5.33×10^{-6}	0.89	2137	67.71
3.5% NaCl + 5×10^{-4} M EH (48 h)	11.97	4.42×10^{-6}	0.91	3632	81.04

https://doi.org/10.1021/acsomega.1c01422
ACS Omega 2021, 6, 14525−14532

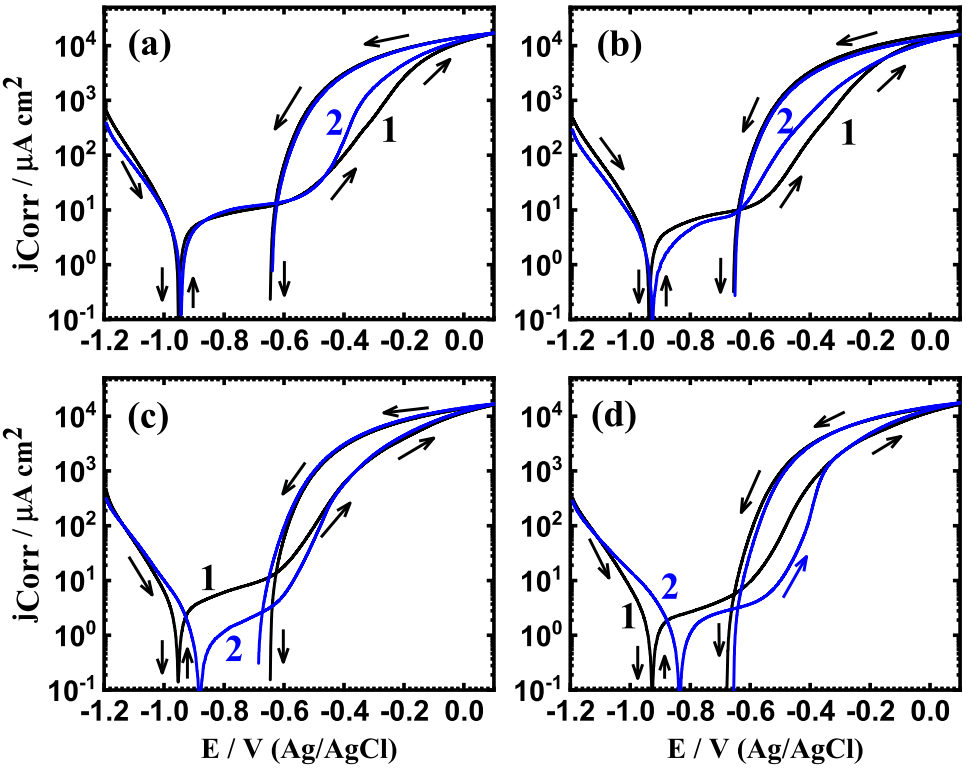

Figure 4. CPP curves for the iron rod after (1) 1 h and (2) 48 h immersion in (a) 3.5% blank NaCl solution and 3.5% NaCl solutions with (b) 5×10^{-5} M EH, (c) 1×10^{-4} M EH, and (d) 5×10^{-4} M EH.

Table 2. Data Obtained from Figure 4 for the Iron Rod in the Different Examined Solutions

solution	β_c (mV/dec)	E_{corr} (mV)	β_a (mV/dec)	j_{corr} (μA/cm^2)	R_p (Ω cm^2)	R_{corr} (mmpy)	IE (%)
3.5% NaCl + 0.0 M EH (1 h)	80	−945	115	3.2	641.03	0.0823	
3.5% NaCl + 5×10^{-5} M EH (1 h)	75	−930	120	2.0	1003.3	0.0514	37.55
3.5% NaCl + 1×10^{-4} M EH (1 h)	70	−945	125	1.5	1300.6	0.0386	53.10
3.5% NaCl + 5×10^{-4} M EH (1 h)	65	−925	135	1.0	1766.3	0.0257	68.77
3.5% NaCl + 0.0 M EH (48 h)	70	−940	110	2.1	885.7	0.0540	
3.5% NaCl + 5×10^{-5} M EH (48 h)	65	−925	105	0.75	2327.4	0.0193	64.26
3.5% NaCl + 1×10^{-4} M EH (48 h)	75	−870	115	0.55	3588.5	0.0141	73.89
3.5% NaCl + 5×10^{-4} M EH (48 h)	65	−830	95	0.40	4195.0	0.0103	80.93

increased all resistances (R_S and R_P) for iron, and this influence was boosted by augmentation of EH concentration. The presence of Q (CPEs) with the values of its "n" exponent varying between 0.8 and 0.9, indicated that Q can be considered as twofold layer capacitors with some porosity.

The impedance (Z_{CPE}) and admittance (Y_{CPE}) of a CPE are defined as follows[45]

$$Z_{CPE} = (1/Y_0)\,(j\omega)^{-n} \quad (2)$$

$$Y_{CPE} = Y_0(j\omega)^n \quad (3)$$

where Y_0 is the modulus, ω is the angular frequency, j is the imaginary unit, and n is the phase.

The values of Y_Q (listed in Table 1) decrease when EH is present in the chloride solution and with increasing EH concentration. This can be attributed to the reduction of the capacitive impacts via the reduction in the local dielectric constant along with the growth in the thickness of the electrical double layer. EIS results subsequently boost the claim that the adsorption of EH molecules increases the inhibition of the iron surface; the adsorption process increases with the increment in EH concentrations. This suggestion is also supported by the increase of the IE% values with the increase of EH concentrations. It is worth mentioning that prolonging the immersion time to 48 h increases the inhibition efficiency of EH, particularly at a high concentration (5×10^{-4} M).

3.2. Cyclic Polarization (CPP) Data. Polarization, CPP, investigations were performed to report the corrosion reactions for the iron rod in the chloride solutions without and with EH added. Figure 4 displays the polarization measurements obtained for the iron rod after (1) 1 and (2) 48 h exposure in (a) 3.5% blank NaCl solutions and 3.5% NaCl solutions with (b) 5×10^{-5}, (c) 1×10^{-4}, and (d) 5×10^{-4} M EH. The corrosion current values (j_{corr}), corrosion potential (E_{corr}), anodic, β_a, and cathodic β_c slopes, corrosion rate (R_{corr}), and polarization resistance (R_P) were obtained as reported in earlier studies.[25−27] The values of all of these parameters are listed in Table 2. The values of IE% were also calculated from polarization curves as per the following equation[6]

$$IE\% = \frac{j^{i}_{corr} - j^{0}_{corr}}{j^{0}_{corr}} \times 100 \quad (4)$$

https://doi.org/10.1021/acsomega.1c01422
ACS Omega 2021, 6, 14525−14532

Here, j_{corr}^{i} and j_{corr}^{0} are the corrosion current densities for the iron rod in the chloride solution with and without EH molecules, respectively.

Figure 4 clarifies that the current in the cathodic side decreased until it reached the values of j_{corr}, after which the current increased in the anodic branch. The cathodic reaction for iron at these conditions was reported[6−8] to be a reduction of oxygen as follows

$$2H_2O + O_2 + 4e^- \rightarrow 4OH^- \quad (5)$$

On the other hand, the reaction in the anodic branch was reported to be the active dissolution of metallic iron to a ferrous cation, followed by the appearance of a passive region due to iron hydroxide and then oxide layer formation as follows[7]

$$Fe^0 = Fe^{2+} + 2e^- \quad (6)$$

$$Fe^0 + 1/2\ O_2 + H_2O \rightarrow Fe(OH)_2 \quad (7)$$

Owing to the instability of the formed $Fe(OH)_2$, it is transformed to an iron oxide, which leads to the appearance of a long passive region. This region is due to the slow increase in current values accompanied by the increment of the potential in a less negative direction. Transformation of the hydroxide into an oxide can be shown by the following reaction[6]

$$1/2\ O_2 + 3Fe(OH)_2 \rightarrow Fe_3O_4 + 3H_2O \quad (8)$$

The current abruptly increases again due to the breakdown of the formed oxide film on the surface during passivation, which motivates the occurrence of pitting corrosion as well. The following reactions may take place with positive potential increment and attack of the chloride ions[6−8,46]

$$Fe\ (s) + 2Cl^-(aq) = FeCl_2(s) + 2e^- \quad (9)$$

$$FeCl_2(s) = FeCl_2(interface) \rightarrow FeCl_2(aq) \quad (10)$$

$$FeCl_2(s) + Cl^-(aq) = FeCl_3(s) + e^- \quad (11)$$

$$FeCl_3(s) = FeC1_3(interface) = FeCl_3(aq) \quad (12)$$

In reality, the presence of a hysteresis loop confirms the occurrence of pitting corrosion, where the currents in the forward direction are less than their values in the back scan direction. It is well known that the severity of pitting corrosion increases with increasing size of the hysteresis loop.

The polarization curves (Figure 4) and Table 2 indicate that 5×10^{-5} M EH reduced the cathodic and anodic currents and the values of j_{corr} and R_{corr}, which increased the R_P value. This effect increases on increasing the EH concentration to 1×10^{-4} M and further to 5×10^{-4} M. The highest IE% value was obtained at 5×10^{-4} M. Prolonging the immersion to 48 h before measurement promotes the EH efficiency, as seen in Table 2. Moreover, an increase in immersion time minimizes the degree of corrosion as a result of the thickening of an oxide film and/or the formation of a corrosion product layer. Whenever the thickness of the formed film increases, the degree of corrosion by the chloride solution decreases. In addition, the availability of EH in the solutions leads to the adsorption of its molecules onto the external surface of the iron rod, thus preventing corrosion. This is emphasized in the data listed in Table 2, as j_{corr} and R_{corr} diminished, while the values of IE% and R_P increased with increase in EH concentration. Increment of EH concentration also decreases the pitting corrosion degree. In comparison to other organic compounds, EH can be regarded as a good corrosion inhibitor.[6−8,45,47−50]

3.3. Change of Current with Time Measurements. The change of current versus time after 1 and 48 h for the chloride solution without/with EH was performed. These experiments were carried out to report the influence of EH concentration on the pitting corrosion of the iron rod. Figure 5a shows the

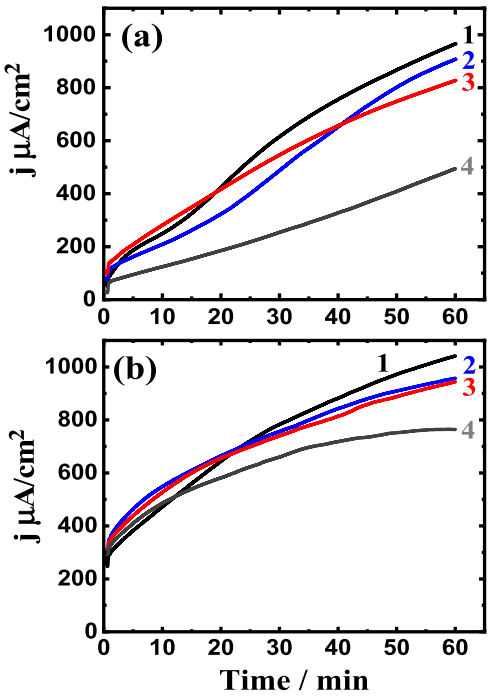

Figure 5. Current−time curves collected at −475 mV (Ag/AgCl) for the iron rod immersed for (a) 1 h and (b) 48 h in 3.5% NaCl solutions containing (1) 0.0 EH, (2) 5×10^{-5} M EH, (3) 1×10^{-4} M EH, and (4) 5×10^{-4} M EH.

current−time curves collected at −475 mV (Ag/AgCl) for the iron rod in 3.5% NaCl solutions containing (1) 0.0 EH, (2) 5×10^{-5} EH, (3) 1×10^{-4} EH, and (4) 5×10^{-4} M EH after 1 h immersion. The same experiments were performed after 48 h, and the curves are plotted in Figure 5b. It was observed that the initial current obtained for the iron rod in all solutions, both after 1 h (Figure 5a) and 48 h (Figure 5b), recorded low values. Perhaps, this occurred because of oxide film formation during the immersion of the iron electrode prior to application of the potential. An increase in the time of potential application enhances the output current for all samples, confirming the occurrence of pitting corrosion. The most elevated current values were obtained for the iron rod in solution containing no EH. Besides, the continuous increment of the current values, which were recorded for the iron rod in 3.5% NaCl blank solution, indicated that both uniform and pitting corrosion have occurred. Here, the dissolution of iron into ferrous ions happens as per eq 6. Furthermore, at the applied potential value, the surface of the iron rod reacts with Cl^- of the solution to form $FeCl_2$ as in eq 9. The $FeCl_2$ surface film transfers to the $FeCl_3$ surface film. Mixed films of $FeCl_2$ and $FeCl_3$ move to the interface and finally to the solution via eqs 10−12, respectively.

At 5×10^{-5} M EH (Figure 5a, curve 2), the absolute value of the obtained current decreased due to the increase in the degree of uniform corrosion. Furthermore, an increase in EH concentration to 1×10^{-4} M (Figure 5a, curve 3) resulted in

https://doi.org/10.1021/acsomega.1c01422
ACS Omega 2021, 6, 14525−14532

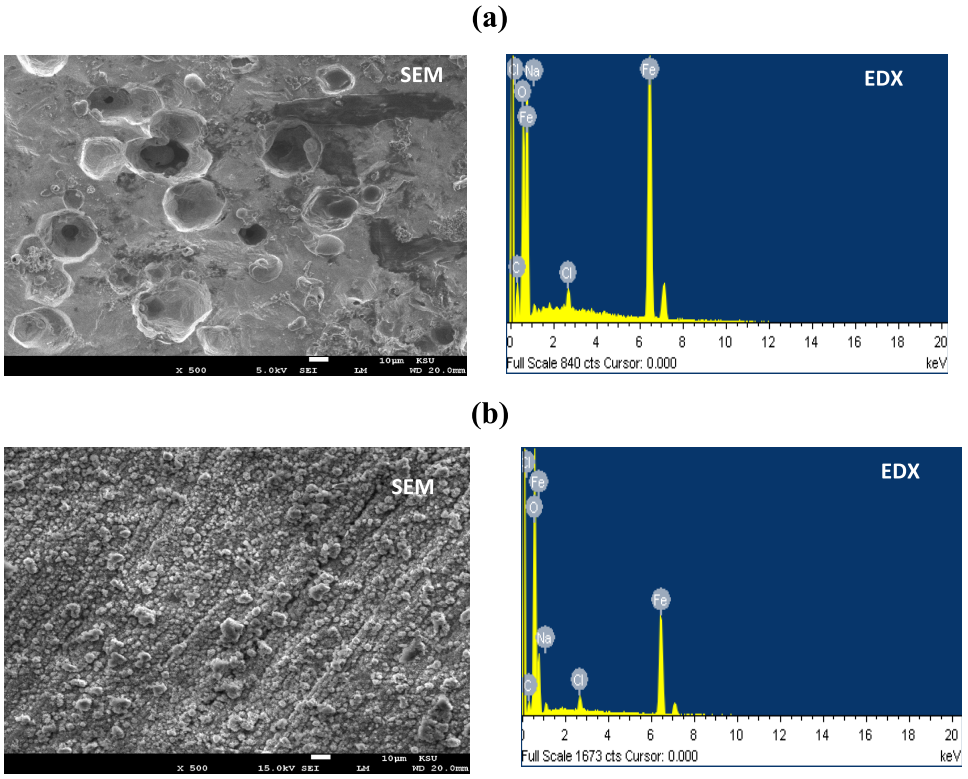

Figure 6. SEM micrographs and EDX spectra collected after holding the potential at −475 mV for 1 h (Ag/AgCl) for the iron surface that was immersed in (a) 3.5% NaCl and (b) 3.5% NaCl + 1×10^{-4} M EH solutions for 48 h before measurement.

lower currents, particularly with expansion of the potential application period. Increment in the concentration of EH to 5×10^{-4} M (Figure 5a curve 4) led to the decrease of the current to the least values. This affirmed that the presence of EH molecules restrained the consumption of iron metal, and this impact was improved through an increase in the concentrations of EH in the chloride solution.

After 48 h exposure (Figure 5b), the change of current showed almost similar behavior to those acquired after 1 h (Figure 5a), where there was a steady increase in its value with time for the iron rod in all solutions. The most elevated currents were registered for the iron rod in the NaCl blank solution, while the presence of EH subsequently diminished the absolute current, which reduced further on increasing EH concentration. This is on the grounds that EH molecules get adsorbed on the outer surface of iron and diminish the corrosive attack of chloride solution.

3.4. SEM/EDX Analysis. To explore the morphology and the elements existing on the outer surface of the iron rod after being corroded in the chloride solution in the presence and absence of the EH compound, SEM analysis and EDX investigation were performed. Figure 6 displays the SEM images and EDX spectra that were obtained after the iron rod was immersed in (a) 3.5% NaCl and (b) 3.5% NaCl + 1×10^{-4} M EH solutions for 48 h before stepping the potential to −475 mV (Ag/AgCl) for 60 min. The SEM graph exhibits so many wide pits that resulted from the harsh effect of the chloride ions along with the active applied potential value. The element contents (atomic %) on the iron surface recorded by EDX analysis were 75.44% Fe, 14.26% O, 8.11% C, 1.26% Cl, and 0.93% Na. The highest percentage is obtained for Fe, followed by O, which suggests that the surface may develop an iron oxide film as per eqs 7 and 8. The presence of low and almost equal amounts of Cl and Na suggests that some NaCl salt may be adsorbed on the iron surface.

The SEM image shown in Figure 6b clearly portrays that the outer surface is completely covered with an inhibitor layer and/or corrosion products, in addition to the absence of any pits. The atomic percentages of the discovered elements on the surface of the iron rod (given by EDX analysis) were as follows: 56.98% Fe, 35.40% O, 4.65% C, 1.55% Cl, and 1.42% Na. The percentage of Fe here is excessively less, while that of O is too high in contrast to that revealed by Figure 6a. The surface is more passivated because of the presence of EH molecules. The low percentage of Na and Cl proves the presence of a thin adsorbed layer of NaCl salt on the surface of the iron rod. The SEM images and EDX profile are in good agreement with the impedance, CPP, and chronoamperometric electrochemical estimations.

4. CONCLUSIONS

The corrosion of iron in 3.5% NaCl solution and its inhibition by ethanedihydrazide (EH) molecules have been reported and the outcomes can be concluded as follows:

- EIS data indicated that the molecules of EH can inhibit corrosion of iron via enhancing its corrosion resistance
- CPP measurements revealed that EH mitigates corrosion of iron in NaCl solution by suppressing the values of j_{corr} and R_{corr} and magnifying the R_p values for iron
- Chronoamperometric results obtained at −475 mV (Ag/AgCl) showed that the presence of EH decreases the possibility of pitting corrosion and reduces the values of absolute currents with the increase in time
- The inhibitive impact of EH was found to increase with the increase in its concentration from 5×10^{-5} to 1×10^{-4} M and further to 5×10^{-4} M

https://doi.org/10.1021/acsomega.1c01422
ACS Omega 2021, 6, 14525−14532

- Prolonging the exposure time from 1 to 48 h prevents corrosion of iron in NaCl solutions and increases the inhibition efficiency of EH, particularly at its high concentrations
- SEM/EDX outcomes agree well with the data obtained by the electrochemical techniques; all data clearly presented that the degree of pitting corrosion is higher in the case of NaCl blank solution, while the availability of EH decreases the occurrence of pitting.

AUTHOR INFORMATION

Corresponding Author

Ayman H. Ahmed − *Chemistry Department, College of Science and Arts, Jouf University, Gurayat, Saudi Arabia; Department of Chemistry, Faculty of Science, Al-Azhar University, Cairo, Egypt*; Email: ahfahmi@ju.edu.sa

Authors

El-Sayed M. Sherif − *Center of Excellence for Research in Engineering Materials (CEREM), College of Engineering, King Saud University, Al-Riyadh 11421, Saudi Arabia*

Hany S. Abdo − *Center of Excellence for Research in Engineering Materials (CEREM), College of Engineering, King Saud University, Al-Riyadh 11421, Saudi Arabia; Mechanical Design and Materials Department, Faculty of Energy Engineering, Aswan University, Aswan 81521, Egypt;* orcid.org/0000-0002-7260-639X

Ehab Said Gad − *Chemistry Department, College of Science and Arts, Jouf University, Gurayat, Saudi Arabia; Department of Chemistry, Faculty of Science, Al-Azhar University, Cairo, Egypt*

Complete contact information is available at: https://pubs.acs.org/10.1021/acsomega.1c01422

Notes

The authors declare no competing financial interest.

ACKNOWLEDGMENTS

The authors extend their appreciation to the Deanship of Scientific Research at Jouf University for funding this work through research grant No (DSR2020-05-412).

REFERENCES

(1) Tristijanto, H.; Ilman, M. N.; TriIswanto, P. Corrosion inhibition of welded of X−52 steel pipelines by sodium molybdate in 3.5% NaCl solution. *Egypt. J. Pet.* **2020**, *29*, 155−162.

(2) Dastgheib, A.; Attar, M. M.; Zarebidaki, A. Evaluation of corrosion inhibition of mild steel in 3.5wt% NaCl solution by cerium nitrate. *Met. Mater. Int.* **2020**, *26*, 1634−2642.

(3) Matter, E. A.; Kozhukharov, S.; Machkova, M.; Kozhukharov, V. Electrochemical studies on the corrosion inhibition of AA2024 aluminium alloy by rare earth ammonium nitrates in 3.5% NaCl solutions. *Mater. Corros.* **2013**, *64*, 408−414.

(4) Macedo, M. C. S. S.; Barcia, O. E.; Da Silva, E. C.; Mendes, J. D.; Mattos, O. R. Corrosion inhibition of iron in NaCl 3.5% by some derivatives imidazole. *J. Electrochem. Soc.* **2012**, *159*, No. C160.

(5) Aslam, R.; Mobin, M.; Aslam, J.; Lgaz, H. Sugar based N, N′didodecyl - N, N′ digluconamideethylenediamine gemini surfactant as corrosion inhibitor for mild steel in 3.5% NaCl solution-effect of synergistic KI additive. *Sci. Rep,* **2018**, *8*, No. 3690.

(6) Sherif, E.-S. M.; Erasmus, R. M.; Comins, J. D. In situ raman spectroscopy and electrochemical techniques for studying corrosion and corrosion inhibition of iron in sodium chloride solutions. *Electrochim. Acta* **2010**, *55*, 3657−3663.

(7) Sherif, E.-S. M. Effects of 5-(3-aminophenyl)-tetrazole on the inhibition of unalloyed iron corrosion in aerated 3.5% sodium chloride solutions as a corrosion inhibitor. *Mater. Chem. Phys.* **2011**, *129*, 961−967.

(8) Sherif, E.-S. M. Corrosion and corrosion inhibition of pure iron in neutral chloride solutions by 1,1'-thiocarbonyldiimidazole. *Int. J. Electrochem. Sci.* **2011**, *6*, 3077−3092.

(9) Zhu, H.; Li, X.; Lu, X.; Chen, X.; Li, J.; Han, X.; Ma, X.; Hu, Z. Intra-/inter-molecular synergistic inhibition effect of sulfonate surfactant and 2-benzothiazolethiol on carbon steel corrosion in 3.5% NaCl solution. *Corros. Sci.* **2021**, *182*, No. 109291.

(10) Fayomi, O. S. I.; Akande, I. G. Corrosion mitigation of aluminium in 3.65% NaCl medium using hexamine. *J. Bio. Tribo. Corros.* **2019**, *5*, No. 23.

(11) Sherif, E.-S. M. corrosion inhibition in chloride solutions of iron by 3-amino-1,2,4-triazole- 5-thiol and 1,1'-thiocarbonyldiimidazole. *Int. J. Electrochem. Sci.* **2012**, *7*, 4834−4846.

(12) Zhang, Z.; Wang, F.; Liu, Y.; Wu, S.; Li, W.; Sun, W.; Guod, D.; Jiang, J. Molecule adsorption and corrosion mechanism of steel under protection of inhibitor in a simulated concrete solution with 3.5% NaCl. *RSC Adv.* **2018**, *8*, 20648.

(13) Shahzad, K.; Sliem, M. H.; Shakoor, R. A.; Radwan, A. B.; Kahraman, R.; Umer, M. A.; Manzoor, U.; Abdullah, A. M. Electrochemical and thermodynamic study on the corrosion performance of API X120 steel in 3.5% NaCl solution. *Sci. Rep.* **2020**, *10*, No. 4314.

(14) Velrani, S.; Jeyaprabha, B.; Prakash, P. Inhibition of mild steel corrosion in 3.5% NaCl medium using 1-butyl-3-methylimidazolium chloride. *Int. J. Innovative Sci. Eng. Technol.* **2014**, *1*, 57−69.

(15) ArockiaSelvi, J.; Kamaraj, P.; Arthanareeswari, M.; PushpaMalini, T.; Mohanapriya, S.; Subasree, N. Effect of cetylpyridinium chloride on corrosion inhibition of mild steel in chloride environment. *Mater. Today: Proc.* **2019**, *14*, 264−270.

(16) Othman, N. K.; Yahya, S.; Ismail, M. C. Corrosion inhibition of steel in 3.5%NaCl by rice straw extract. *J. Ind. Eng. Chem.* **2019**, *70*, 299−310.

(17) Suarez, M.; Delgado, F.; Yanez, F.; León, J. B.; Prinzio, A. D.; González, W. A. Study of the electrochemical behavior of mango extract as a corrosion inhibitor of carbon steels by varying the pH of the electrolytic medium. *Acta Microsc.* **2020**, *29*, 10−18.

(18) Nazari, M. H.; Shihab, M. S.; Havens, E. A.; Shi, X. Mechanism of corrosion protection in chloride solution by an apple-based green inhibitor: experimental and theoretical studies. *J. Infrastruct. Preserv. Resilience* **2020**, *1*, 1−19.

(19) Shyamvarnan, B.; Shanmugapriya, S.; Selvi, J. A.; Kamaraj, P.; Mohankumar, R. Corrosion inhibition effect of *elettaria cardamomum* extract on mild steel in 3.5% NaCl medium. *Mater. Today: Proc.* **2021**, *40*, S192−S197.

(20) Pradityana, A.; Sulistijono; Shahab, A.; Noerochim, L.; Susanti, D. Inhibition of corrosion of carbon steel in 3.5% nacl solution by *myrmecodia pendans* extract. *Int. J. Corros.* **2016**, *2016*, No. 6058286.

(21) Dahmani, M.; Et - Touhami, A.; Al − Deyab, S. S.; Hammouti, B.; Bouyanzer, A. Corrosion inhibition of C38 steel in 1M HCl: a comparative study of black pepper extract and its isolated piperine. *Int. J. Electrochem. Sci.* **2010**, *5*, 1060−1069.

(22) Amin, M. A.; Abd El − Rehim, S. S.; El - Sherbini, E. E.; Bayoumi, R. S. The inhibition of low carbon steel corrosion in hydrochloric acid solutions by succinicacid part I. weight loss, polarization, EIS, PZC, EDX and ESM studies. *Electrochim. Acta* **2007**, *52*, 3588−3599.

(23) Thomas, J. G. N. *5th European Symposium on Corrosion Inhibitors*; University of Ferrara: Ferrara, Italy, 1981; p 453.

(24) Tadros, A. B.; Abdel-Naby, Y. Inhibition of the acid corrosion of steel by 4-amino-3-hydrazino-5-thio-1,2,4-triazoles. *J. Electroanal. Chem.* **1988**, *246*, 433−439.

(25) Subramanyam, N. C.; Sheshadri, B. S.; Mayanna, S. M. Thiourea and substituted thioureas as corrosion inhibitors for aluminum in sodium nitrite solution. *Corros. Sci.* **1993**, *34*, 563−571.

(26) Sherif, E.-S. M.; Ahmed, A. H. Synthesizing new hydrazone derivatives and studying their effects on the inhibition of copper

corrosion in sodium chloride solutions. *Synth. React. Inorg., Met.-Org., Nano-Met. Chem.* **2010**, *40*, 365−372.
(27) Ahmed, A. H.; Hassan, A. M.; Gumaa, H. A.; Mohamed, B. H.; Eraky, A. M.; Omran, A. A. Copper(II)-oxaloyldihydrazone complexes: Physico-chemical studies; energy band gap and inhibition evaluation of free oxaloyldihydrazones toward the corrosion of copper metal in acidic medium. *Arabian J. Chem.* **2019**, *12*, 4287−4302.
(28) Ahmed, A. H.; Hassan, A. M.; Gumaa, H. A.; Mohamed, B. H.; Eraky, A. M. Physicochemical studies on some selected oxaloyldihydrazones and their novel palladium(II) complexes along with using oxaloyldihydrazones as corrosion resistants. *Inorg. Nano-Met. Chem.* **2017**, *47*, 1652−1663.
(29) Ahmed, A. H.; Hassan, A. M.; Gumaa, H. A.; Mohamed, B. H.; Eraky, A. M. Mn^{2+}-complexes of N,O-dihydrazone: structural studies, indirect band gap energy and corrosion inhibition on aluminum in acidic medium. *J. Chil. Chem. Soc.* **2018**, *63*, 4159−4168.
(30) Shanbhag, A. V.; Venkatesha, T. V.; Prabhu, R. A.; Kalkhambkar, R. G.; Kulkarni, G. M. Corrosion inhibition of mild steel in acidic medium using hydrazide derivatives. *J. Appl. Electrochem.* **2008**, *38*, 279−287.
(31) Singh, A. K.; Chugh, B.; Singh, M.; Thakur, S.; Pani, B.; Guo, L.; Kaya, S.; Serdaroglu, G. Hydroxy phenyl hydrazides and their role as corrosion impeding agent: A detail experimental and theoretical study. *J. Mol. Liq.* **2021**, *330*, No. 115605.
(32) Ichchou, I.; Larabi, L.; Rouabhi, H.; Harek, Y.; Fellah, A. Electrochemical evaluation and DFT calculations of aromatic sulfonohydrazides as corrosion inhibitors for XC38 carbon steel in acidic media. *J. Mol. Struct.* **2019**, *1198*, No. 126898.
(33) Chugh, B.; Singh, A. K.; Chaouiki, A.; Salghi, R.; Thakur, S.; Pani, B. A comprehensive study about anti-corrosion behavior of pyrazine carbohydrazide: Gravimetric, electrochemical, surface and theoretical study. *J. Mol. Liq.* **2020**, *299*, No. 112160.
(34) Kumbhar, C. G.; Sadasivan, N. Co(II), Ni(II) and Cu(1I) complexes of oxalic, malonic and terephthalic dihydrazides. *Def. Sci. J.* **1982**, *35*, 113−117.
(35) Sherif, E.-S. M.; Abdo, H. S.; Latief, F. H.; Alharthi, N. H.; Zein El Abedin, S. Fabrication of Ti−Al−Cu new alloys by inductive sintering, characterization, and corrosion evaluation. *J. Mater. Res. Technol.* **2019**, *8*, 4302−4311.
(36) Sherif, E.-S. M.; Latief, F. H.; Abdo, H. S.; Alharthi, N. H. Electrochemical and spectroscopic study on the corrosion of ti−5al and ti−5al−5cu in chloride solutions. *Met. Mater. Int.* **2019**, *25*, 1511−1520.
(37) Feliu, S., Jr Electrochemical impedance spectroscopy for the measurement of the corrosion rate of magnesium alloys: brief review and challenges. *Metals* **2020**, *10*, No. 775.
(38) Uwaya, G. E.; Fayemi, O. E.; Sherif, E. M.; Junaedi, H.; Ebenso, E. E. Synthesis, electrochemical studies, and antimicrobial properties of Fe_3O_4 nanoparticles from callistemon viminalis plant extracts. *Materials* **2020**, *13*, No. 4894.
(39) Okpara, E. C.; Fayemi, O. E.; Sherif, E. M.; Junaedi, H.; Ebenso, E. E. Green wastes mediated zinc oxide nanoparticles: synthesis, characterization and electrochemical studies. *Materials* **2020**, *13*, No. 4241.
(40) Kuriakose, N.; Kakkassery, J. T.; Raphael, V. P.; Shanmughan, S. K. electrochemical impedance spectroscopy and potentiodynamic polarization analysis on anticorrosive activity of thiophene-2-carbaldehyde derivative in acid medium. *Indian J. Mater. Sci.* **2014**, *2014*, No. 124065.
(41) Sherif, E. M.; Park, S.-M. Inhibition of copper corrosion in 3.0% NaCl by n-phenyl-1,4-phenylenediamine. *J. Electrochem. Soc.* **2005**, *152*, No. B428.
(42) Sherif, E. M.; Park, S.-M. Effects of 2-amino-5-ethylthio-1,3,4-thiadiazole on copper corrosion as a corrosion inhibitor in aerated acidic pickling solutions. *Electrochim. Acta* **2006**, *51*, 6556−6562.
(43) Sherif, E. M.; Park, S.-M. Inhibition of copper corrosion in acidic pickling solutions by N-phenyl-1,4-phenylenediamine. *Electrochim. Acta* **2006**, *51*, 4665−4673.
(44) Sherif, E. M.; Park, S.-M. 2-Amino-5-ethyl-1,3,4-thiadiazole as a corrosion inhibitor for copper in 3.0% nacl solutions. *Corros. Sci.* **2006**, *48*, 4065−4079.
(45) Zhang, Z.; Chen, S.; Li, Y.; Li, S.; Wang, L. A study of the inhibition of iron corrosion by imidazole and its derivatives self-assembled films. *Corros. Sci.* **2009**, *51*, 291−300.
(46) Li, W.; Nobe, K.; Pearlstein, A. J. Potential/current oscillations and anodic film characteristics of iron in concentrated chloride solutions. *Corros. Sci.* **1990**, *31*, 615−620.
(47) Sabirneeza, A. A. F.; Geethanjali, R.; Subhashini, S. Polymeric corrosion inhibitors for iron and its alloys: a review. *Chem. Eng. Commun.* **2015**, *202*, 232−244.
(48) Allaoui, M.; Rahim, O.; Sekhri, L. Electrochemical study on corrosion inhibition of iron in acidic medium by moringa oleifera extract. *Orient. J. Chem.* **2017**, *33*, 637−646.
(49) El-Haddad, M. A. M.; Radwan, A. B.; Sliem, M. H.; Hassan, W. M. I.; Abdullah, A. M. Highly efcient eco-friendly corrosion inhibitor for mild steel in 5M HCl at elevated temperatures: experimental & molecular dynamics study. *Sci. Rep.* **2019**, *9*, No. 3695.
(50) Shainy, K. M.; Ammal, P. R.; Unni, K. N.; Benjamin, S.; Joseph, A. surface interaction and corrosion inhibition of mild steel in hydrochloric acid using pyoverdine, an eco-friendly biomolecule. *J. Bio. Tribo. Corros.* **2016**, *2*, No. 20.

https://doi.org/10.1021/acsomega.1c01422
ACS Omega 2021, 6, 14525−14532